Defraeye T, Blocken B, Derome D, Nicolai B, Carmeliet J. 2012. Convective heat and mass transfer modelling at air-porous material interfaces: overview of existing methods and relevance. ***Chemical Engineering Science*** 74: 49–58

# Convective heat and mass transfer modelling at air-porous material interfaces: overview of existing methods and relevance

Thijs Defraeye [a *], Bert Blocken [b], Dominique Derome [c], Bart Nicolai [a], Jan Carmeliet [d,e]

[a] *VCBT / MeBioS, Department of Biosystems, Katholieke Universiteit Leuven, Willem de Croylaan 42, 3001 Heverlee, Belgium*
[b] *Building Physics and Services, Eindhoven University of Technology, P.O. Box 513, 5600 Eindhoven, The Netherlands*
[c] *Department of Civil and Mechanical Engineering, Swiss Federal Laboratories for Materials Testing and Research (Empa), Überlandstrasse 129, 8600 Dübendorf, Switzerland*
[d] *Chair of Building Physics, Swiss Federal Institute of Technology Zurich (ETHZ), Wolfgang-Pauli-Strasse 15, 8093 Zürich, Switzerland*
[e] *Laboratory for Building Science and Technology, Swiss Federal Laboratories for Materials Testing and Research (Empa), Überlandstrasse 129, 8600 Dübendorf, Switzerland*

**Keywords**
convective transfer coefficient; conjugate modelling; porous material; computational fluid dynamics; drying; air flow

**Abstract**
Accurate predictions of convective heat and mass transfer at air-porous material interfaces are essential in many engineering applications, one example being optimisation of industrial drying processes with respect to energy consumption and product quality. For porous-material modelling purposes, simplified convective transfer coefficients (CTCs) are often used to avoid explicit air-flow modelling. Alternatively, conjugate models have been introduced recently and are being more widely used. Conjugate modelling has the advantage that it does not require the use of CTCs or of the heat and mass transfer analogy. Instead, these CTCs can be identified a-posteriori. In this study, an overview of the existing methods to predict convective heat and mass transfer at air-porous material interfaces is given, with a specific focus on conjugate modelling. The improved accuracy of this approach is indicated based on two case studies, namely hygroscopic loading and convective drying. A large spatial and temporal variability of the CTCs is found by means of conjugate modelling. This approach provides increased accuracy, which is especially relevant for complex flow problems, such as in industrial drier systems. However, the sensitivity to the convective boundary conditions can be limited in some cases, e.g. for hygroscopic loading. Instead of improving accuracy significantly here, conjugate modelling will rather impose an additional modelling effort, which often requires conjugate model code development as these models are not readily available. Before embarking on a conjugate modelling study, it is advised to perform a sensitivity analysis with respect to the convective boundary conditions: in some cases, sufficient accuracy can be obtained using empirical CTCs from literature.

[*] Corresponding author. Tel.: +32 (0)16321618; fax: +32 (0)16322966.
E-mail address: thijs.defraeye@biw.kuleuven.be

**Nomenclature**

| | |
|---|---|
| $D_{PM}$ | thickness of porous material (m) |
| $D_{GB}$ | thickness of gypsum board (m) |
| $g_{v,w}$ | convective water vapour flux at the air-porous material interface/wall (kg/m²s) |
| H | channel height (m) |
| $L_{PM}$ | length of porous material (m) |
| $p_{v,ref}$ | reference vapour pressure (Pa) |
| $p_{v,w}$ | vapour pressure at the air-porous material interface/wall (Pa) |
| $q_{c,w}$ | convective heat flux at the air-porous material interface/wall (W/m²) |
| Re | Reynolds number |
| $R_{BL}$ | vapour diffusion resistance of boundary layer (m/s) |
| $R_{GB}$ | vapour diffusion resistance of gypsum board (m/s) |
| t | time (s) |
| $t_{tot}$ | total time (s) |
| T | temperature (K or °C) |
| $T_{ref}$ | reference temperature (K or °C) |
| $T_w$ | temperature at the air-porous material interface/wall (K or °C) |
| $T_{wb}$ | wet bulb temperature (K or °C) |
| $U_b$ | bulk air speed (m/s) |
| x | coordinate (m) |
| y | coordinate (m) |

*Abbreviations*

| | |
|---|---|
| avg | surface-averaged |
| CDRP | constant drying rate period |
| CFD | computational fluid dynamics |
| CHTC | convective heat transfer coefficient |
| CMTC | convective mass transfer coefficient |
| CTC | convective transfer coefficient |
| DDRP | decreasing drying rate period |
| EPDM | effective penetration depth model |
| HAM | heat-air-moisture |
| RH | relative humidity |
| TP | transition period |

*Greek symbols*

| | |
|---|---|
| $\delta_{v,GB}$ | water vapour diffusion coefficient of gypsum board (s) |

*Subscripts*

| | |
|---|---|
| BL | boundary layer |
| CDRP | constant drying rate period |
| GB | gypsum board |
| PM | porous material |
| ref | reference condition |
| v | water vapour |
| w | wall/air-porous material interface |

## 1. Introduction

Convective heat and mass transfer from porous materials is of interest for many engineering applications, such as: (1) a wide range of industrial drying applications (Mujumdar, 2006; Putranto et al., 2011), e.g. the production of building materials (concrete, brick, gypsum board, etc.; e.g. Suresh et al., 2001; Murugesan et al., 2001), food processing (Scheerlinck et al., 2000, 2001; Hoang et al., 2000, 2003; Kaya et al., 2006; De Bonis and Ruocco, 2008; Lamnatou et al., 2009; Lamnatou et al., 2010) or wood and paper production (Erriguible et al., 2006; Younsi et al., 2008; Kowalski, 2010; Kowalski and PawLowski, 2011). The vast majority of these drying processes still occur convectively and are very energy consuming operations. Optimisation of the drying process is particularly required to enhance processing efficiency, in terms of energy usage and production time, without compromising the product quality, for example by excessive shrinkage or warping; (2) outdoor hygrothermal analysis of building envelopes and components from the perspective of design of durable building envelope systems and preservation of cultural heritage. Here knowledge on the convective exchange is required, for example to analyse thermal performance (e.g. Palyvos, 2008; Blocken et al., 2009; Defraeye et al., 2010, 2011a, 2011b), to determine the drying of facades wetted by wind-driven rain (e.g. Blocken and Carmeliet, 2004; Blocken et al., 2007), or to analyse several physical, chemical and biological weathering processes (e.g. Poupeleer et al., 2006a, 2006b); (3) indoor hygrothermal analysis related to indoor climate and comfort, mould growth risk, moisture buffering (Steeman et al., 2009a; Carmeliet et al., 2011), preservation of valuable historical objects such as paintings (Steeman et al., 2009b), energy consumption related to (de)humidification of the air, etc.; (4) analysis of volatile organic compound (VOC) emissions to indoor air (Yang et al., 2001). Since the majority of the aforementioned applications involve moisture transport (i.e. liquid and vapour), this paper will focus on water ($H_2O$) as the mass transfer component. A generalisation to other substances is straightforward.

In addition to experimental research on these convective transfer mechanisms (e.g. Belhamri and Fohr, 1996; Iskra et al., 2009), several numerical modelling approaches have been developed to model the coupled heat and moisture transport in porous materials, such as pore network models (e.g. Prat, 1993; Carmeliet et al., 1999; Yiotis et al., 2001) or macroscopic models (e.g. Ben Nasrallah and Perre, 1988; Cloutier et al, 1992; Janssen et al., 2007; Moonen et al., 2010). In these models, the convective heat and mass exchange with the environment is usually modelled by means of convective heat and mass transfer coefficients, i.e. CHTCs and CMTCs, respectively. These convective transfer coefficients (CTCs) relate the convective heat and moisture flux normal to the wall ($q_{c,w}$ and $g_{v,w}$), i.e. the air-porous material interface, to the difference between the wall temperature ($T_w$) or vapour pressure at the wall ($p_{v,w}$) and a reference temperature ($T_{ref}$) or vapour pressure ($p_{v,ref}$), for example the approach flow conditions:

$$\mathrm{CHTC} = \frac{q_{c,w}}{T_w - T_{ref}} \tag{1}$$

$$\mathrm{CMTC} = \frac{g_{c,w}}{p_{v,w} - p_{v,ref}} \tag{2}$$

The fluxes are assumed positive away from the porous material. CTCs however account for the convective exchange in a quite simplified way (Defraeye et al., 2012): (1) CTCs are often estimated by means of empirical correlations with the air speed, where these correlations were mostly derived for simplified configurations, such as flat plates; (2) The spatial variation of CTCs along the surface and especially their temporal variation are often not accounted for; (3) CMTCs are often estimated from CHTCs by using the heat and mass transfer analogy (Chilton and Colburn, 1934), which only applies under strict conditions (no radiation, no coupling between heat and mass transfer, analogous boundary conditions, etc.); (4) CTCs are strongly dependent on the reference conditions ($T_{ref}$ and $p_{v,ref}$), but the location where these are evaluated is generally chosen rather arbitrary for complex flow problems. Due to these simplifications, the use of such CTCs can seriously compromise the accuracy of the air-side convective heat and mass transfer predictions for certain applications, one of them being convective drying of porous materials (Defraeye et al., 2012).

Since convective heat and mass transfer from porous materials involves transport both in the air and in the porous material, it is actually a conjugate transport problem and should be considered likewise in numerical modelling, thus by accounting for two domains: the air and the porous material. Thus, instead of using the well-established CTCs, explicitly resolving heat and mass transport in the air, in addition to resolving heat and mass transport in the porous material, is advised since it is inherently more accurate. Several approaches towards such conjugate modelling of convective exchange processes have been proposed in the past two decades and will be discussed in this paper. Note however that a reduced accuracy of the imposed convective boundary conditions (e.g. by using CTCs) in porous-material modelling does not necessarily disturb a reliable simulation (Belhamri and Fohr, 1996), for example when heat and mass transport at the porous material-side governs the transport kinetics. The level of complexity with which the air-side convective exchange processes have to be accounted for in numerical models and the impact on the accuracy of the simulation results are thus important questions to be answered when dealing with convective transfer problems.

This study aims to clarify some of the aforementioned issues regarding convective transfer predictions, and their impact on numerical modelling. First, an overview of different modelling approaches and previous studies for convective heat and mass transfer for porous materials is given, with a specific focus on conjugate modelling, and their advantages and limitations are discussed. Second, the relevance of accurate numerical modelling of convective exchange processes is indicated by means of two (conjugate) case studies, namely hygroscopic loading and convective drying of porous materials. Third, a discussion on convective heat and mass transfer predictions and the need for conjugate modelling is presented.

## 2. Overview of numerical modelling approaches

Numerically solving convective heat and mass transfer problems implies that both the transport in the air and in the porous material are modelled (and solved), which can be done at several levels of complexity in both media. For porous-material modelling, the following approaches are commonly used:

- Effective penetration depth model (EPDM, Cunningham, 1992).
- Shrinking core models, also called receding front models (e.g. Luikov, 1975; Hashimoto et al., 2003).
- Macroscopic continuum models for coupled multiphase heat and mass transport in porous materials. Three approaches exist: (1) the phenomenological approach (Philip and De Vries, 1957; Luikov, 1966); (2) the approach relying on mixture theory (e.g. Bowen, 1980); (3) the volume-averaging approach at the microscopic scale (see Whitaker, 1977, 1998).
- Pore-network models (e.g. Prat, 1993; Carmeliet et al., 1999; Yiotis et al., 2001), of which an overview can be found in Blunt (2001) and Prat (2002).

From the perspective of porous-material models, the degree of conjugate modelling is determined by the way in which the heat and mass transport in the air is accounted for. The most commonly used approaches are:

- <u>Non-conjugate approach</u>. CTCs from literature are used, which have been determined analytically or (semi-)empirically (i.e. by experimental or numerical studies) as a correlation with the air speed, generally for simplified configurations such as flat plates. Often, the focus of such CTC research is rather on CHTCs, where the CMTCs are still often determined from the heat and mass transfer analogy. An overview of CHTC predictions for flat plates by wind-tunnel experiments is given by Palyvos (2008), within the context of solar collector research. Defraeye et al. (2011a) provided an overview of CHTC predictions for bluff bodies immersed in turbulent boundary layers (e.g. buildings). Although these CTCs account for the influence of the air-flow field to some extent, for example by correlation with the air speed or by including a spatial variation over the surface, there will always exist (often significant) dissimilarities with the specific flow problem of interest, with respect to the flow and scalar fields (geometry, boundary conditions, …), because actual aerodynamic problems, such as wind flow around buildings and in urban areas, are generally very complex (e.g. Blocken and Carmeliet, 2004; van Hooff and Blocken, 2010; Gousseau et al., 2011). Thereby, the use of such CTCs is considered to be a non-conjugate approach.
- <u>Semi-conjugate approach</u>. The air-side heat and mass transport for the specific flow problem under study is accounted for by applying case-related CTCs, which can be done in several ways:
    - By including a case-specific spatial variation of the CTCs over the porous surface, which is determined a-priori by a separate flow field calculation (e.g. Kaya et al., 2006). These CTCs can be obtained by solving the flow analytically, i.e. solving boundary-layer equations, or solving the flow numerically, i.e. solving the Navier-Stokes equations (by computational fluid dynamics, CFD). Since the specific flow, thermal and concentration fields are not solved in a transient manner, this approach is considered to be semi-conjugate.
    - By including a temporal variation of the CTCs, namely a dependency of CTCs on the moisture content at the surface (Chen and Pei, 1989). Although the specific flow, thermal and concentration fields are not solved explicitly in this case, they are to some extent related to the transient heat and mass transport at the surface, by which this approach is also considered to be semi-conjugate.
- <u>Conjugate approach</u>. The heat and mass transport in the air and in the porous material are solved simultaneously in a transient way, i.e. the flow field is solved using boundary-layer equations or Navier-Stokes equations. Continuity of heat and mass fluxes and temperature and mass fractions (e.g. water vapour) at every location on the interface is thus required. Thereby the need for using CTCs is avoided, but instead they can be determined a-posteriori from the conjugate calculation. As such, the spatial and temporal variability of heat and mass transfer in both air flow and porous material can be fully taken into account, and the spatial and temporal variability of the CTCs can be identified. Note that some conjugate models solve air flow assuming a quasi steady-state flow field, based on the assumption that time scales for convection in the air are much smaller than those for heat and mass transfer in the porous material. Thereby, only heat and mass transfer in the air is solved in a transient way (not momentum transfer), which is however only valid for non-buoyant flows since for buoyant flows the flow field also varies in time, as heat acts as an active scalar.

Most numerical research on transport in porous materials was devoted to non-conjugate modelling, i.e. by using simplified CTCs, as the focus was rather on the aforementioned porous-material modelling approaches (EPDM: Steeman et al., 2009a; shrinking core models: Hashimoto et al., 2003; macroscopic models: Ben Nasrallah and Perre, 1988; Ilic and Turner, 1989; Turner and Ilic, 1990; Prat, 1991; Kallel et al., 1993; Boukadida and Ben Nasrallah, 1995; Zhang et al., 1999; Boukadida et al., 2000; Nijdam et al., 2000; Haghi, 2001; Lu et al., 2005; Kocaefe et al., 2006; Younsi et al., 2006; Janssen et al., 2007; Alexandri and Jones, 2007; Lu and Shen, 2007; Murugesan et al., 2008; pore-network models: Laurindo and Prat, 1996; Laurindo and Prat, 1998; Le Bray and Prat, 1999; Yiotis et al., 2001; Plourde and Prat, 2003; Yiotis et al., 2005; Yiotis et al., 2006; Prat, 2007; Surasani et al., 2008).

Numerical models which apply a conjugate or semi-conjugate approach are much scarcer. An overview of the available models for convective heat and mass transfer applications with water as the mass transfer component, to the current knowledge of the authors, is given in Table 1. For drying applications, only conjugate models for convective drying are considered, e.g. no microwave drying. In addition, water is considered to be only in the liquid or gas state, thus freeze drying (e.g. Nam and Song, 2007) is also not included. Note that, apart from applications for moisture transport, such a conjugate approach has also been applied for VOC transfer for indoor environments (e.g. Yang et al., 2001) and for building energy simulation programs (Chen and Srebric, 2000; Zhai et al., 2002; Mora et al., 2003; Zhai and Chen, 2004; Zhai, 2006), where air-flow modelling (e.g. with CFD) is used to provide more accurate thermal boundary conditions for the interior and exterior of the building envelope. CFD was already often applied for such convective transfer predictions in the past (e.g. Karava et al., 2011; Defraeye et al., 2012). The following remarks can be made regarding the (semi-)conjugate models presented in Table 1:

- Conjugate modelling is a relatively recent development, as the majority of the progress has been made during the past decade.
- Mainly 2D conjugate modelling has been performed.
- Although these (semi-)conjugate models were mainly developed for drying applications, this does not necessarily imply that the material is fully saturated.
- Radiation is usually not accounted for in these models.
- Validation of these conjugate models is often not performed. When performed, experimental data from other researchers is often used, and the transport in the porous material and in the air is usually validated separately.

Often, the reason for applying non-conjugate modelling instead of the (semi-)conjugate approach is the additional modelling effort that has to be performed: (1) The air-flow domain also has to be solved, which inherently implies an increased computational cost; (2) As (semi-)conjugate models are not yet commercially available, they consist of in-house developed codes in which an air-flow model has been programmed or where a coupling procedure with an existing air-flow model (e.g. CFD software) was established. A more detailed evaluation of the convective exchange processes by means of a conjugate approach has shown to enhance the numerical predictive accuracy, e.g. for convective drying processes (e.g. Erriguible et al., 2006; Defraeye et al., 2012). However, as discussed above, the impact of the imposed convective boundary conditions on the heat and mass transfer from the porous material is not always significant, by which non-conjugate modelling is sufficiently accurate for certain applications. The necessity of accurate convective transfer modelling is illustrated in the next section by two numerical case studies.

## 3. Relevance of accurate surface convective transfer predictions

### 3.1. Background

Before describing both case studies, the general characteristics of convective heat and mass exchange of porous materials with external air flow are briefly discussed. This discussion is written from the perspective of quasi-saturated porous materials, thus for drying processes, due to their relevance for many industrial applications (Mujumdar, 2006). Here, water is considered as the mass transfer component.

A typical drying process is depicted in Figure 1, with respect to mass flow rate ($g_{v,w}$), surface temperature ($T_w$) and relative humidity at the surface ($RH_w$). After an initial transition period (TP), the material experiences the constant drying rate period (CDRP), given that the air-material interface remains wet. The CDRP is characterised by a relative humidity (RH) of quasi 100% at the surface, a constant drying rate and a constant material temperature, which is equal to the wet bulb temperature ($T_{wb}$) if no radiative heat flows at the surface and (conductive) heat flows from the interior of the porous material are present. In this case, the convective heat supply to the interface is quasi entirely used for the evaporation of water, which requires latent heat for the phase change from liquid water to vapour.

As evaporation occurs at the air-porous material interface during the CDRP, the drying rate is determined by the air-flow conditions and not by the porous-material transport properties. Nevertheless, the porous-material transport properties do affect the length of the CDRP, since it is dependent on the supply of liquid to the surface. When the material dries out at the interface, the decreasing drying rate period (DDRP) sets in, which is characterised by a lower drying rate (see Figure 1). During DDRP, the liquid water front recedes from the surface and water, once evaporated, must diffuse out via the “dry” outer porous material layer. This dry layer can be seen as an additional resistance to liquid water transport from the inside of the material. Due to this material resistance, in addition to the boundary-layer resistance, the drying rate of most porous materials during the DDRP is thereby much less sensitive to the convective boundary conditions. This decrease in drying rate is accompanied by a temperature increase since less latent heat is required for the evaporation of water. Also for applications where materials do not contain any liquid water thus where only vapour transport occurs, the convective moisture exchange rate with the environment is usually dominated by the vapour diffusion in the material, rather than by the air-flow field. Note however that the sensitivity of the drying process to convective heat transfer can be pronounced during the DDRP in some cases, as discussed in section 4.

Although the insensitivity of mass transfer from porous materials to the convective boundary conditions during the DDRP is generally known (Mujumdar, 2006), it is often left unacknowledged resulting in too detailed modelling of the convective conditions. For indoor climate analysis for example, high spatial resolution CTCs are often determined as a function of different ventilation system characteristics by means of CFD, although these CTCs are usually not dominating the moisture transport kinetics. Here, accurate and detailed CTCs are actually not essential for the resulting modelling accuracy. In the next section, two case studies illustrate the impact and relevance of convective transfer predictions for numerical modelling of convective heat and mass exchange processes.

### 3.2. Case studies

#### 3.2.1. Configuration

The setup used in both case studies is taken from the study of James et al. (2010). They analysed the hygroscopic buffering of gypsum boards experimentally by means of a small closed-circuit wind-tunnel setup and made a comparison with numerical simulations. The same configuration was also used by Defraeye et al. (2012) to investigate convective drying of a mineral plaster plate numerically. In these studies, a two-dimensional fully-developed laminar channel flow (channel height H = 20.5 mm) is produced over the porous material (length $L_{PM}$ = 500 mm and thickness $D_{PM}$ = 37.5 mm, i.e. 3 gypsum boards of 12.5 mm or a mineral plaster plate of 37.5 mm), which is mounted flush with one of the channel walls. The porous material is insulated (adiabatic conditions) and made impermeable for moisture on its remaining surfaces. This experimental setup is described in detail by Talukdar et al. (2007).

In the present numerical study, this configuration is evaluated for two cases: (1) case 1: the experiment of James et al. (2010), which involves hygroscopic loading of gypsum boards; (2) case 2: the numerical study of Defraeye et al. (2012), which involves convective drying of a capillary saturated mineral plaster plate. In the second case, the only differences with the experiment of James et al. (2010) are the used porous material (mineral plaster) and the initial porous-material moisture content and temperature.

#### 3.2.2. Computational model

The computational model used for the numerical analyses is presented in Figure 2, together with the imposed boundary conditions for both cases. A detailed description of this computational model is given in Defraeye et al. (2012) and is not repeated here. The computational model, its boundary conditions and the material properties are in accordance with the experiment of James et al. (2010) for both cases, except for the porous material type and its initial moisture content and temperature of case 2. For case 1, the gypsum board is initially conditioned at 30% RH and 23.3°C. For case 2, the mineral plaster is assumed to be initially unsaturated, but at capillary saturation moisture content (126 kg/m³) at a temperature of 20.0°C. This temperature is approximately equal to the wet bulb temperature (≈ 20°C for $T_{ref}$ = 23.8°C and $RH_{ref}$ = 71.9% RH). The material properties for the plaster are given in Defraeye et al. (2012); those of gypsum board are given in James et al. (2010). Gypsum board is actually a layered composite material consisting of gypsum and paper liner. In this study, gypsum board is modelled as a single material, in accordance with James et al. (2010), which determined the relevant material properties accordingly.

#### 3.2.3. Numerical simulation

Conjugate modelling implies that both the transport in the air and in the porous material are solved. The air-flow simulations are performed assuming laminar flow, due to the low Reynolds numbers (Re = 1100, see Figure 2), with the commercial computational fluid dynamics (CFD) code Fluent 6.3 (Fluent, 2006), which uses the control volume method. Radiation between the channel walls is not considered because: (1) for case 1, the experiment is nearly isothermal, by which the influence of radiation is quasi negligible; (2) for case 2, the focus of Defraeye et al. (2012) was also on the validity of the heat and mass transfer analogy, which cannot be valid if radiation is taken into account. Note that James et al. (2010) also did not account for radiation and that they used a CHTC which was determined from the CMTC by means of the heat and mass transfer analogy (from Iskra and Simonson, 2007). The porous-material simulations are performed with a non-commercial finite-element porous-material model (or heat-air-moisture (HAM) transport model), called HAMFEM. Detailed numerical modelling information can be found in Janssen et al. (2007). Since two different programs are used for air-flow and porous-material modelling (Fluent 6.3 and HAMFEM), an external coupling protocol between these programs was implemented, where the exchange of boundary conditions between the two programs is performed once every time step. More details on this conjugate model can be found in Defraeye et al. (2012).

In addition, the conjugate modelling approach is compared with porous-material modelling (with HAMFEM) using spatially and temporally constant CTCs, which will be referred to as the constant CTC approach. The applied CTCs for this approach are specified for each case in sections 3.2.4 and 3.2.5.

### 3.2.4. Case 1: Hygroscopic loading of gypsum boards

For a typical hygroscopic loading experiment, the moisture content of a material, achieved at equilibrium with air at a set relative humidity, changes due to exposure to air with a different relative humidity. Hygroscopic loading usually involves only vapour transport, and no liquid transport. Thereby, the material can actually be considered to be in a relatively late state of the DDRP. A nearly isothermal experiment was used by James et al. (2010) to validate different porous-material models (including the porous-material model used in the proposed conjugate model) for hygroscopic loading of 3 gypsum boards, using the wind-tunnel setup described in section 3.2.1. Here, both relative humidity and temperature were measured in between two gypsum boards (using capacitive humidity sensors and thermocouples, respectively), together with the moisture accumulation of the ensemble of boards (using load cells). The conjugate simulation results are compared with the experimental data of James et al. (2010) in Figure 3. Here, the temperature and relative humidity in the middle of the material below the first gypsum board are shown (x = 250 mm, y = -12.5 mm, see Figure 2) as well as the total moisture accumulation in the material. In addition, the results of the constant CTC approach are also included. Here, the spatially and temporally constant CTCs, as determined experimentally by James et al. (2010), were imposed (CHTC = 3.45 W/m²K, CMTC = $2.41 \times 10^{-8}$ s/m). Both the conjugate model and the constant CTC approach seem to predict the relative humidity, temperature and moisture accumulation quite well, i.e. approximately within the experimental uncertainty, and produce very similar results, indicating that no significantly increased accuracy is obtained with the conjugate model.

The good agreement between the porous-material model using constant CTCs and the conjugate model is due to the very small sensitivity of the heat and mass transport to the flow field (James et al., 2010). It was shown by Defraeye et al. (2012) (see also section 3.2.5) however that the (surface-averaged) CTCs used in both approaches actually differed significantly (≈ 50%) for this flat-plate configuration. This low sensitivity to convective vapour transfer originates from the relatively high resistance of gypsum board to vapour transfer ($R_{GB}$), compared to that of the boundary layer ($R_{BL}$). These resistances are compared in Figure 4 as a function of the thickness of the gypsum board ($D_{GB}$) for different RH of the gypsum board. Here, $R_{BL} = CMTC^{-1}$ and $R_{GB} = D_{GB}/\delta_{v,GB}$, where $\delta_{v,GB}$ is the water vapour diffusion coefficient of gypsum board. $R_{BL}$ quickly becomes much smaller than $R_{GB}$ with increasing $D_{GB}$. As a result, for many porous materials, the vapour uptake/release kinetics are mainly determined by the material itself and not by the air flow, resulting in a good agreement between conjugate and constant CTC approaches. Actually, the discrepancies with experiments were found to result mainly from experimental uncertainties on the material properties which are used in the porous-material model (James et al., 2010). For these types of problems, where the largest resistances to moisture transfer are located in the porous material (equivalent to the DDRP), (semi-)conjugate modelling clearly does not contribute significantly to an increased modelling accuracy.

### 3.2.5. Case 2: Convective drying of a mineral plaster plate

For convective drying of a capillary saturated porous flat plate (mineral plaster), Defraeye et al. (2012) compared porous-material modelling using constant (spatial and temporal) CTCs with conjugate modelling. The CTCs used by the constant CTC approach were obtained from surface-averaged CHTC values from CFD simulations, combined with the analogy to determine the CMTC (CHTC = 5.34 W/m²K, CMTC = $3.77 \times 10^{-8}$ s/m). The drying rate, surface temperature and relative humidity at the surface of the two approaches are shown as a function of dimensionless time in Figure 5. Due to their spatial variability for the conjugate approach, these parameters are presented at specific locations on the porous-material surface, namely at x = 0, 0.25 and 0.5 m, but the surface-averaged $g_{v,w}$ is also presented. The drying rates are scaled with the drying rate during the CDRP from the constant CTC approach ($g_{v,w,CDRP}$).

For the constant CTC approach, the CDRP and DDRP (see Figure 1) can clearly be distinguished. For the conjugate approach, the surface-averaged drying rate shows a much shorter CDRP, which is found to be related to the two-dimensional drying effect: the surface near the leading edge dries out first and quickly, by which the total drying rate quickly decreases, while the remaining part of the surface dries out later. A CDRP can be distinguished at specific locations on the surface, where its duration increases with distance from the leading edge. Distinct peaks in the drying rate appear, which approximately correspond with the moment in time where the surface dries out locally (RH < 100%, see Figure 5c). These peaks result from the downstream progression of the drying front with time (see Defraeye et al., 2012), where the drying front indicates the separation between the dried-out and still-wet part of the interface. When considering the surface-averaged drying rates of both approaches in Figure 5a, the sensitivity to the convective boundary conditions is clearly less pronounced during the DDRP, due to the additional material resistance.

As the conjugate approach does not require CTCs to represent the convective boundary conditions, it allows calculating the CTCs a-posteriori, by which their temporal and spatial variability can be identified. The resulting CMTCs are shown in Figure 6 as a function of dimensionless time and location on the interface by means of a contour plot. A distinct spatial variation can be noticed, with higher values closer to the leading edge. In addition, a strong temporal variability can be noticed, especially at the transition from CDRP to DDRP, i.e. when the surface locally dries out. The temporal variation indicates that CTCs are not only intrinsically related to the specific flow field, which is responsible for the spatial CTC variation, but that they are also dependent on the transient temperature and moisture distribution in the flow field (boundary layer) and at the air-porous material interface.

## 4. Discussion

An alternative to porous-material modelling using constant (spatial and/or temporal) CTCs has become more popular in the past decades, namely conjugate modelling. Conjugate modelling allows accounting for spatial and temporal variations in convective boundary conditions and thereby it circumvents the use of CTCs, which actually quantify the air-side heat and mass transfer in a rather simplified way. As shown in section 3, the need for detailed modelling of convective boundary conditions is however strongly dependent on the moisture transport characteristics of the porous material. In general, conjugate modelling will improve simulation accuracy during the CDRP and the transition to the DDRP, i.e. when the surface is (partially) wet, since then the air flow mainly determines the drying rate. During the DDRP however, the impact of the CTC predictions on the accuracy of exchange processes was shown to be more limited (section 3.2.4), as the internal vapour resistance of the porous material dictates the liquid water removal rate from the material, and (semi-)conjugate modelling does not seem to be required. Instead of accurate modelling of the convective boundary conditions, material characterisation related to liquid and vapour transport is more critical here.

However, convective heat transfer can play a significant role throughout the entire drying process (also during the DDRP) due to its impact on the convective moisture exchange of the porous material with the environment, particularly for strong non-isothermal problems. The reasons for this are that: (1) convective heat exchange determines, in part, the latent heat supply required for moisture removal from the porous material; (2) the boundary-layer resistance for heat transfer often lies much closer to the heat transfer resistance of typical porous materials, by which the sensitivity to convective heat transfer becomes larger; (3) mass transfer in porous materials can be thermally driven. Although highly accurate convective mass transfer predictions are not required during the DDRP, and probably in any hygroscopic loading case, conjugate modelling of convective heat (not mass) transfer could have a pronounced effect on the predicted heat and mass exchange. The impact of the convective heat flow component on drying processes will however be strongly case dependent, as it is a result from the specific heat balance at the surface, which includes radiation amongst others. Therefore it is difficult to state general conclusions in this matter. Such an assessment however inherently requires conjugate modelling, and the suggestion of guidelines for such an assessment is a topic of future research.

When evaluating a conjugate heat and mass exchange problem numerically, it is thus advised to evaluate a-priori the sensitivity of the exchange processes to the convective boundary conditions, e.g. by comparing boundary-layer and material resistances. From this analysis, the required degree of detail for the specification of the convective boundary conditions can be determined. In some studies, conjugate modelling is required but is not applied because a conjugate model is not available or in order to limit the computational expense. In this case, it is strongly suggested to account for the spatial variation of the CTCs when performing porous-material modelling, for example by determining the CHTC by means of a CFD study and the corresponding CMTC using the analogy. Furthermore, for flow configurations which have a more applied nature than the ones presented in this paper, e.g. in actual industrial driers, flow fields and exchange processes will be more complex due to the presence of strong radiation, buoyancy, turbulence, etc. Here, the increased accuracy from conjugate modelling will often be even more pronounced. Turbulence, for example, will usually enhance transfer rates compared to laminar flow, but is highly dependent on the specific flow field, flow configuration and flow history. Thereby, the resulting ensemble of turbulence structures (eddies) is very case specific, i.e. unique. This case specific nature of turbulent flow, and thus of turbulent convective transfer (CTCs), hence increases the need for a conjugate assessment of (convective) heat and mass transfer from porous materials, compared to laminar flow.

Another significant advantage of the conjugate modelling approach, often left unacknowledged, is that it does not rely on the heat and mass transfer analogy. As this analogy is only valid under strict conditions (see Defraeye et al., 2012), no radiation amongst others, it cannot be used in principle for the majority of the conjugate problems in engineering, such as drying (Chen et al., 2002). However, it is applied regularly and it is often found to be sufficiently accurate. On the other hand, conjugate modelling is an appropriate tool to investigate the validity of the analogy under different conditions.

Finally, conjugate models (and related required software) are not yet widely known or used, due to their limited (commercial) availability amongst others. Thereby, the conjugate studies performed up to now considered simplified configurations (see Table 1) using in-house developed codes or coupling between/with existing codes. In this stage of active model development, validation of such conjugate models with detailed experiments is imperative. Such experiments are however very scarce (e.g. Belhamri and Fohr, 1996) and are still an active topic of ongoing research (Murugesan et al., 2001). Preferably, future experiments should be specifically designed for conjugate model validation:

as shown in section 3.2.4, some experiments do not have a large sensitivity to convective exchange, by which they are not appropriate because they mainly validate the porous-material model.

## 5. Conclusions

In this study, an overview was given of existing methods to model convective heat and mass transfer at air-porous material interfaces for porous-material modelling purposes. Instead of using well-established convective transfer coefficients (CTCs), conjugate modelling is clearly becoming a more widely used, and inherently more accurate, approach. Based on two case studies, namely hygroscopic loading and convective drying, the improved accuracy of this approach was indicated. Conjugate modelling has the advantage that it does not require CTCs, but it can identify them a-posteriori. As shown in this study, a large spatial and temporal CTC variability can be found. Furthermore, the use of the heat and mass transfer analogy is not required. These advantages are especially relevant for complex flow problems, such as in industrial drier systems. However, the sensitivity to the convective boundary conditions can be limited in some cases, e.g. during the DDRP. Instead of significantly improving the accuracy here, conjugate modelling will rather impose an additional modelling effort, which sometimes even requires conjugate model code development as these models are not readily (commercially) available. In such cases, the focus should rather be on ensuring the accuracy of porous-material modelling. Before embarking on a conjugate modelling study, which often implies CFD modelling, it is therefore advised to perform a-priori a sensitivity analysis with respect to the convective boundary conditions. In some cases, sufficient accuracy can be obtained using empirical CTCs from literature.


## Acknowledgements

Thijs Defraeye is a postdoctoral fellow of the Research Foundation – Flanders (FWO) and acknowledges its support. Financial support by the Research Foundation – Flanders (project FWO G.0603.08) and K.U.Leuven (project OT 08/023) is also gratefully acknowledged. These sponsors had no involvement in: the study design, in the collection, analysis and interpretation of data; in the writing of the manuscript; and in the decision to submit the manuscript for publication.


## References


Alexandri, E., Jones, P., 2007. Developing a one-dimensional heat and mass transfer algorithm for describing the effect of green roofs on the built environment: Comparison with experimental results. Building and Environment 42 (8), 2835-2849.

Belhamri, A., Fohr, J.P., 1996. Heat and mass transfer along a wetted porous plate in an airstream. AIChE Journal 42 (7), 1833-1843.

Ben Nasrallah, S., Perre, P., 1988. Detailed study of a model of heat and mass transfer during convective drying of porous media. International Journal of Heat and Mass Transfer 31 (5), 957-967.

Blocken, B., Carmeliet, J., 2004. A review of wind-driven rain research in building science. Journal of Wind Engineering and Industrial Aerodynamics 92 (13), 1079-1130.

Blocken, B., Roels, S., Carmeliet, J., 2007. A combined CFD-HAM approach for wind-driven rain on building facades. Journal of Wind Engineering and Industrial Aerodynamics 95 (7), 585-607.

Blocken, B., Defraeye, T., Derome, D., Carmeliet, J., 2009. High-resolution CFD simulations of forced convective heat transfer coefficients at the facade of a low-rise building. Building and Environment 44 (12), 2396-2412.

Blunt, M.J., 2001. Flow in porous media - pore-network models and multiphase flow. Current Opinion in Colloid & Interface Science 6 (3), 197-207.

Boukadida, N., Ben Nasrallah, S., 1995. Two dimensional heat and mass transfer during convective drying of porous media. Drying Technology 13 (3), 661-694.

Boukadida, N., Ben Nasrallah, S., Perre, P., 2000. Mechanism of two-dimensional heat and mass transfer during convective drying of porous media under different drying conditions. Drying Technology 18 (7), 1367-1388.

Bowen, R.M, 1980. Incompressible porous media models by use of the theory of mixtures. International Journal of Engineering Science 18 (9), 1129-1148.

Carmeliet, J., Blocken, B., Defraeye, T., Derome, D., 2011. Moisture phenomena in whole building performance prediction, in: Hensen, J.L.M., Lamberts, R. (Eds.), Building Performance Simulation for Design and Operation. Taylor and Francis, London, UK.

Carmeliet, J., Descamps, F., Houvenaghel, G., 1999. A multiscale network model for simulating moisture transfer properties of porous media. Transport in Porous Media 35, 67-88.

Chandra Mohan, V.P., Talukdar, P., 2010. Three dimensional numerical modeling of simultaneous heat and moisture transfer in a moist object subjected to convective drying. International Journal of Heat and Mass Transfer 53 (21-22), 4638-4650.

Chen, P., Pei, D.C.T., 1989. A mathematical model of drying processes. International Journal of Heat and Mass Transfer 32 (2), 297-310.

Chen, Q., Srebric, J., 2000. Application of CFD tools for indoor and outdoor environment design. International Journal on Architectural Science 1 (1), 14-29.

Chen, X.D., Lin, S.X.Q., Chen, G., 2002. On the ratio of heat and mass transfer coefficient for water evaporation and its impact upon drying modelling. International Journal of Heat and Mass Transfer 45 (21), 4369-4372.
Chilton, T.H., Colburn, A.P., 1934. Mass transfer (absorption) coefficients. Industrial and Engineering Chemistry 26 (11), 1183-1187.
Cloutier, A., Fortin, Y., Dhatt, G., 1992. A wood drying finite element model based on the water potential concept. Drying technology 10 (5), 1151-1181.
Cunningham, M.J., 1992. Effective penetration depth and effective resistance in moisture transfer. Building and Environment 27 (3), 379-386.
De Bonis, M.V., Ruocco, G., 2008. A generalized conjugate model for forced convection drying based on an evaporative kinetics. Journal of Food Engineering 89 (2), 232-240.
Defraeye, T., Blocken, B., Carmeliet, J., 2010. CFD analysis of convective heat transfer at the surfaces of a cube immersed in a turbulent boundary layer. International Journal of Heat and Mass Transfer 53 (1-3), 297-308.
Defraeye, T., Blocken, B., Carmeliet, J., 2011a. Convective heat transfer coefficients for exterior building surfaces: Existing correlations and CFD modelling. Energy Conversion and Management 52 (1), 512-522.
Defraeye, T., Blocken, B., Carmeliet, J., 2011b. An adjusted temperature wall function for turbulent forced convective heat transfer for bluff bodies in the atmospheric boundary layer. Building and Environment 46 (11), 2130-2141.
Defraeye, T., Blocken, B., Carmeliet, J., 2012. Analysis of convective heat and mass transfer coefficients for convective drying of a porous flat plate by conjugate modelling. International Journal of Heat and Mass Transfer 55 (1-3), 112-124.
Dolinskiy, A.A., Dorfman, A.S.H., Davydenko, B.V., 1991. Conjugate heat and mass transfer in continuous processes of convective drying. International Journal of Heat and Mass Transfer 34 (11), 2883-2889.
Erriguible, A., Bernada, P., Couture, F., Roques, M., 2005. Modeling of heat and mass transfer at the boundary between a porous medium and its surroundings. Drying Technology 23 (3), 455-472.
Erriguible, A., Bernada, P., Couture, F., Roques, M., 2006. Simulation of convective drying of a porous medium with boundary conditions provided by CFD. Chemical Engineering Research and Design 84 (2), 113-123.
Gousseau, P., Blocken, B., Stathopoulos, T., van Heijst, G.J.F., 2011. CFD simulation of near-field pollutant dispersion on a high-resolution grid: a case study by LES and RANS for a building group in downtown Montreal. Atmospheric Environment 45 (2), 428-438.
Fluent Inc., Fluent 6.3 User's Guide, Lebanon - New Hampshire, USA, 2006.
Haghi, A.K., 2001. A mathematical model of the drying process. Acta Polytechnica 41 (3), 20-23.
Hashimoto, A., Stenström, S., Kameoka, T., 2003. Simulation of convective drying of wet porous materials. Drying Technology 21 (8), 1411-1431.
Hoang, M., Verboven, P., Baelmans, M., Nicolai, B., 2003. A continuum model for airflow, heat and mass transfer in bulk of chicory roots. Transactions of the ASAE 46 (6), 1603-1611.
Hoang, M., Verboven, P., De Baerdemaeker, J., Nicolaï, B., 2000. Analysis of the air flow in a cold store by means of computational fluid dynamics. International Journal of Refrigeration 23 (2), 127-140.
Ilic, M., Turner, I.W., 1989. Convective drying of a consolidated slab of wet porous material. International Journal of Heat and Mass Transfer 32 (12), 2351-2362.
Iskra, C.R., James, C., Talukdar, P., Simonson, C.J., 2009. Convective mass transfer coefficients for gypsum and wood panelling. Journal of ASTM International 6 (4), 1-18.
Iskra, C.R., Simonson, C.J., 2007. Convective mass transfer coefficient for a hydrodynamically developed airflow in a short rectangular duct. International Journal of Heat and Mass Transfer 50 (11-12), 2376-2393.
James, C., Simonson, C.J., Talukdar, P., Roels, S., 2010. Numerical and experimental data set for benchmarking hygroscopic buffering models. International Journal of Heat and Mass Transfer 53 (19-20), 3638-3654.
Janssen, H., Blocken, B., Carmeliet, J., 2007. Conservative modelling of the moisture and heat transfer in building components under atmospheric excitation. International Journal of Heat and Mass Transfer 50 (5-6), 1128-1140.
Kallel, F., Galanis, N., Perrin, B., Javelas, R., 1993. Effects of moisture on temperature during drying of consolidated porous materials. Transactions of the ASME: Journal of Heat Transfer 115, 724-733.
Karava, P., Jubayer, C.M., Savory, E., 2011. Numerical modelling of forced convective heat transfer from the inclined windward roof of an isolated low-rise building with application to photovoltaic/thermal systems. Applied Thermal Engineering 31 (11-12), 1950-1963.
Kaya, A., Aydin, O., Dincer, I., 2006. Numerical modeling of heat and mass transfer during forced convection drying of rectangular moist objects. International Journal of Heat and Mass Transfer 49 (17-18), 3094-3103.
Kocaefe, D., Younsi, R., Chaudry, B., Kocaefe, Y., 2006. Modeling of heat and mass transfer during high temperature treatment of aspen. Wood Science and Technology 40 (5), 371-391.
Kowalski, S.J., 2010. Control of mechanical processes in drying. Theory and experiment. Chemical Engineering Science 65 (2), 890-899.
Kowalski, S.J., Pawlowski, A., 2011. Intermittent drying of initially saturated porous materials. Chemical Engineering Science 66 (9), 1893-1905.
Lamnatou, Chr., Papanicolaou, E., Belessiotis, V., Kyriakis, N., 2009. Conjugate heat and mass transfer from a drying rectangular cylinder in confined air flow. Numerical Heat Transfer, Part A: Applications 56 (5), 379-405.

Lamnatou, Chr., Papanicolaou, E., Belessiotis, V., Kyriakis, N., 2010. Finite-volume modelling of heat and mass transfer during convective drying of porous bodies - Non-conjugate and conjugate formulations involving the aerodynamic effects. Renewable Energy 35 (7), 1391-1402.
Laurindo, J.B., Prat, M., 1996. Numerical and experimental network study of evaporation in capillary porous media. Phase distributions. Chemical Engineering Science 51 (23), 5171-5185.
Laurindo, J.B., Prat, M., 1998. Numerical and experimental network study of evaporation in capillary porous media. Drying rates. Chemical Engineering Science 53 (12), 2257-2269.
Le Bray, Y., Prat, M., 1999. Three-dimensional pore network simulation of drying in capillary porous media. International Journal of Heat and Mass Transfer 42 (22), 4207-4224.
Lu, T., Jiang, P., Shen, S., 2005. Numerical and experimental investigation of convective drying in unsaturated porous media with bound water. Heat and Mass Transfer 41 (12), 1103-1111.
Lu, T., Shen, S.Q., 2007. Numerical and experimental investigation of paper drying: Heat and mass transfer with phase change in porous media. Applied Thermal Engineering 27 (8-9), 1248-1258.
Luikov, A.V., 1966. Heat and Mass Transfer in Capillary-Porous Bodies, first ed. Pergamon Press, New York, USA.
Luikov, A.V., 1975. Systems of differential equations of heat and mass transfer in capillary-porous bodies. International Journal of Heat and Mass Transfer 18 (1), 1-14.
Masmoudi, W., Prat, M., 1991. Heat and mass transfer between a porous medium and a parallel external flow. Application to drying of capillary porous materials. International Journal of Heat and Mass Transfer 34 (8), 1975-1989.
Moonen, P., Sluys, L.J., Carmeliet, J., 2010. A continuous–discontinuous approach to simulate physical degradation processes in porous media. International Journal for Numerical Methods in Engineering 84 (9), 1009–1037.
Mora, L., Gadgil, A. J., Wurtz, E., 2003. Comparing zonal and CFD model predictions of isothermal indoor airflows to experimental data. Indoor Air 13 (2), 77-85.
Mortensen, L.H., Woloszyn, M., Rode, C., Peuhkuri, R., 2007. Investigation of microclimate by CFD modeling of moisture interactions between air and constructions. Journal of Building Physics 30(4), 279-315.
Mujumdar, A.S. (Editor), 2006. Handbook of Industrial Drying, third ed. Taylor & Francis Group, Boca Raton, USA.
Murugesan, K., Lo, D.C., Young, D.L., Chen, C.W., Fan, C.M., 2008. Convective drying analysis of three-dimensional porous solid by mass lumping finite element technique. Heat and Mass Transfer 44 (4), 401-412.
Murugesan, K., Suresh, H.N., Seetharamu, K.N., Aswatha Narayana, P.A., Sundararajan, T., 2001. A theoretical model of brick drying as a conjugate problem. International Journal of Heat and Mass Transfer 44 (21), 4075-4086.
Nam, J.H., Song, C.S., 2007. Numerical simulation of conjugate heat and mass transfer during multi-dimensional freeze drying of slab-shaped food products. International Journal of Heat and Mass Transfer 50 (23-24), 4891-4900.
Nijdam, J.J., Langrish, T.A.G., Keey, R.B., 2000. A high-temperature drying model for softwood timber. Chemical Engineering Science 55 (18), 3585-3598.
Oliveira, L.S., Fortes, M., Haghighi, K., 1994. Conjugate analysis of natural convective drying of biological materials, Drying Technology 12 (5), 1167-1190.
Oliveira, L.S., Haghighi, K., 1998. Conjugate heat and mass transfer in convective drying of porous media. Numerical Heat Transfer, Part A: Applications 34, 105-117.
Palyvos, J.A., 2008. A survey of wind convection coefficient correlations for building envelope energy systems' modelling. Applied Thermal Engineering 28 (8-9), 801-808.
Philip, J.R., De Vries, D.A., 1957. Moisture movement in porous materials under temperature gradients. Transactions American Geophysical Union 38 (2), 222-232.
Plourde, F., Prat, M., 2003. Pore network simulations of drying of capillary porous media. Influence of thermal gradients. International Journal of Heat and Mass Transfer 46 (7), 1293-1307.
Poupeleer, A.S., Roels, S., Carmeliet, J., Van Gemert, D., 2006a. Diffusion-convection transport of salt solutions in cracked porous building materials. Part 1: Parameters, model description and application to cracks. International Journal for Restoration of Buildings and Monuments 12 (3), 187-204.
Poupeleer, A.S., Roels, S., Carmeliet, J., Van Gemert, D., 2006b. Diffusion-convection transport of salt solutions in cracked porous building materials. Part 2: Analysis of salt transport in cracked bricks and dead ending cracks. International Journal for Restoration of Buildings and Monuments 12 (3), 205-218.
Prat, M., 1991. 2D modelling of drying of porous media: Influence of edge effects at the interface. Drying Technology 9 (5), 1181-1208.
Prat, M., 1993. Percolation model of drying under isothermal conditions in porous media. International Journal of Multiphase Flow 19 (4), 691-704.
Prat, M., 2002. Recent advances in pore-scale models for drying of porous media. Chemical Engineering Journal 86 (1-2), 153-164.
Prat, M., 2007. On the influence of pore shape, contact angle and film flows on drying of capillary porous media. International Journal of Heat and Mass Transfer 50 (7-8), 1455-1468.
Putranto, A., Chen, X.D., Devahastin, S., Xiao, Z., Web, P.A., 2011. Application of the reaction engineering approach (REA) for modeling intermittent drying under time-varying humidity and temperature. Chemical Engineering Science 66 (10), 2149-2156.

Scheerlinck, N., Verboven, P., Stigter, J., De Baerdemaeker, J., Van Impe, J., Nicolai, B., 2000. Stochastic finite element analysis of coupled heat and mass transfer problems with random field parameters. Numerical Heat Transfer Part b -Fundamentals 37 (3), 309-330.
Scheerlinck, N., Verboven, P., Stigter, J., De Baerdemaeker, J., Van Impe, J., Nicolai, B., 2001. A variance propagation algorithm for stochastic heat and mass transfer problems in food processes. International Journal for Numerical Methods in Engineering 51 (8), 961-983.
Steeman, H.J., Janssens, A., Carmeliet, J., De Paepe, M., 2009a. Modelling indoor air and hygrothermal wall interaction in building simulation: Comparison between CFD and a well-mixed zonal model. Building and Environment 44 (3), 572-583.
Steeman, H.J., Van Belleghem, M., Janssens, A., De Paepe, M., 2009b. Coupled simulation of heat and moisture transport in air and porous materials for the assessment of moisture related damage. Building and Environment 44 (10), 2176-2184.
Surasani, V.K., Metzger, T., Tsotsas, E., 2008. Consideration of heat transfer in pore network modelling of convective drying. International Journal of Heat and Mass Transfer 51 (9-10), 2506-2518.
Suresh, H.N., Aswatha Narayana, P.A., Seetharamu, K.N., 2001. Conjugate mixed convection heat and mass transfer in brick drying. Heat and Mass Transfer 37 (2-3), 205-213.
Talukdar, P., Olutmayin, S.O., Osanyintola, O.F., Simonson, C.J., 2007. An experimental data set for benchmarking 1-D, transient heat and moisture transfer models of hygroscopic building materials. Part I: Experimental facility and material property data. International Journal of Heat and Mass Transfer 50 (23-24), 4527-4539.
Turner, I.W., Ilic, M., 1990. Convective drying of a consolidated slab of wet porous material including the sorption region. International Communications in Heat and Mass Transfer 17 (1), 39-48.
van Hooff, T., Blocken, B., 2010. Coupled urban wind flow and indoor natural ventilation modelling on a high-resolution grid: a case study for the Amsterdam ArenA stadium. Environmental Modelling & Software 25(1), 51-65.
Whitaker, S., 1977. Simultaneous heat, mass, and momentum transfer in porous media: A theory of drying. Advances in Heat Transfer 13, 119-203.
Whitaker, S., 1998. Coupled transport in multiphase systems: A theory of drying. Advances in Heat Transfer 31, 1-104.
Yang, X., Chen, Q., Zhang, J.S., Magee, R., Zeng, J., Shaw, C.Y., 2001. Numerical simulation of VOC emissions from dry materials. Building and Environment 36 (10), 1099-1107.
Yiotis, A.G., Stubos, A.K., Boudouvis, A.G., Tsimpanogiannis, I.N., Yortsos, Y.C., 2005. Pore-network modelling of isothemal drying in porous media. Transport in Porous Media 58 (1-2), 63-86.
Yiotis, A.G., Stubos, A.K., Boudouvis, A.G., Yortsos, Y.C., 2001. A 2-D pore-network model of the drying of single-component liquids in porous media. Advances in Water Resources 24 (3-4), 439-460.
Yiotis, A.G., Tsimpanogiannis, I.N., Stubos, A.K., Yortsos, Y.C., 2006. Pore-network study of the characteristic periods in the drying of porous materials. Journal of Colloid and Interface Science 297 (2), 738-748.
Younsi, R., Kocaefe, D., Poncsak, S., Kocaefe, Y., 2006. Thermal modelling of the high temperature treatment of wood based on Luikov's approach. International Journal of Energy Research 30 (9), 699-711.
Younsi, R., Kocaefe, D., Poncsak, S., Kocaefe, Y., 2007. Computational modelling of heat and mass transfer during the high-temperature heat treatment of wood, Applied Thermal Engineering 27 (8-9), 1424-1431.
Younsi, R., Kocaefe, D., Poncsak, S., Kocaefe, Y., Gastonguay, L., 2008. CFD modeling and experimental validation of heat and mass transfer in wood poles subjected to high temperatures: a conjugate approach. Heat and Mass Transfer 44 (12), 1497-1509.
Zeghmati, B., Daguenet, M., Le Palec, G., 1991. Study of transient laminar free convection over an inclined wet flat plate. International Journal of Heat and Mass Transfer 34 (4-5), 899-909.
Zhai, Z., 2006. Applications of Computational Fluid Dynamics in building design: aspects and trends. Indoor and Built Environment 15 (4), 305-313.
Zhai, Z., Chen, Q., Haves, P., Klems, J.H., 2002. On approaches to couple energy simulation and computational fluid dynamics programs. Building and Environment 37 (8-9), 857-864.
Zhai, Z., Chen, Q.Y., 2004. Numerical determination and treatment of convective heat transfer coefficients in the coupled building energy and CFD simulation. Building and Environment 39, 1001-1009.
Zhang, Z., Yang, S., Liu, D., 1999. Mechanism and mathematical model of heat and mass transfer during convective drying of porous materials. Heat Transfer - Asian Research 28 (5), 337-351.

**Figures**

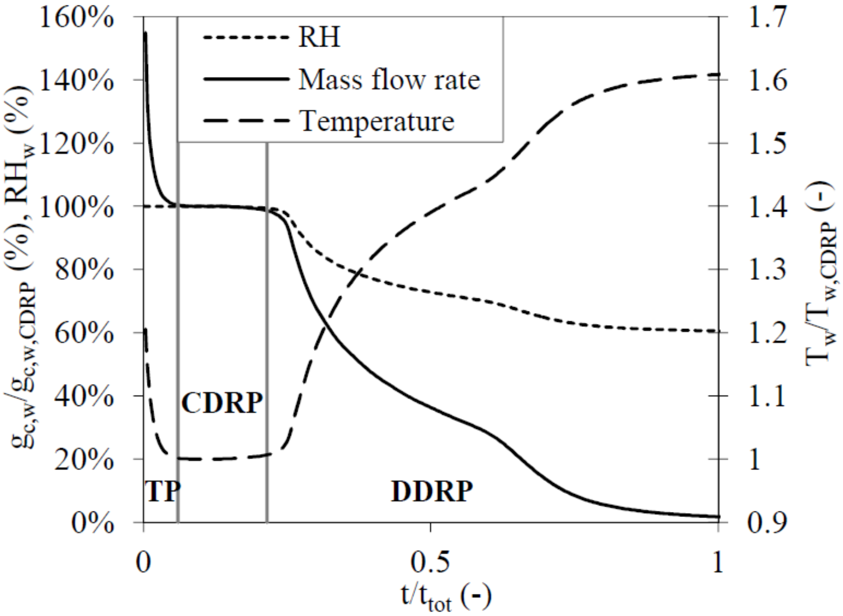


Figure 1. Typical drying rate ($g_{v,w}$), surface temperature ($T_w$) and relative humidity at the surface ($RH_w$) of a porous material during drying, as a function of dimensionless time ($t/t_{tot}$), obtained from a numerical simulation with a porous-material model. The different drying periods are indicated. For $g_{v,w}$ and $T_w$, scaling is performed using the values during the CDRP (temperatures are in °C). The time is scaled with the total simulation time ($t_{tot}$).

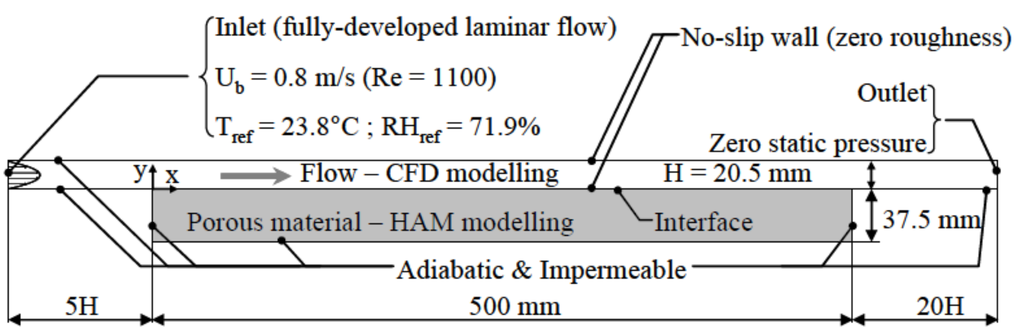


Figure 2. Two-dimensional computational model and boundary conditions for numerical analyses (not to scale, taken from Defraeye et al. 2012; $U_b$: bulk air speed; H: channel height; Re: Reynolds number based on $U_b$ and H).

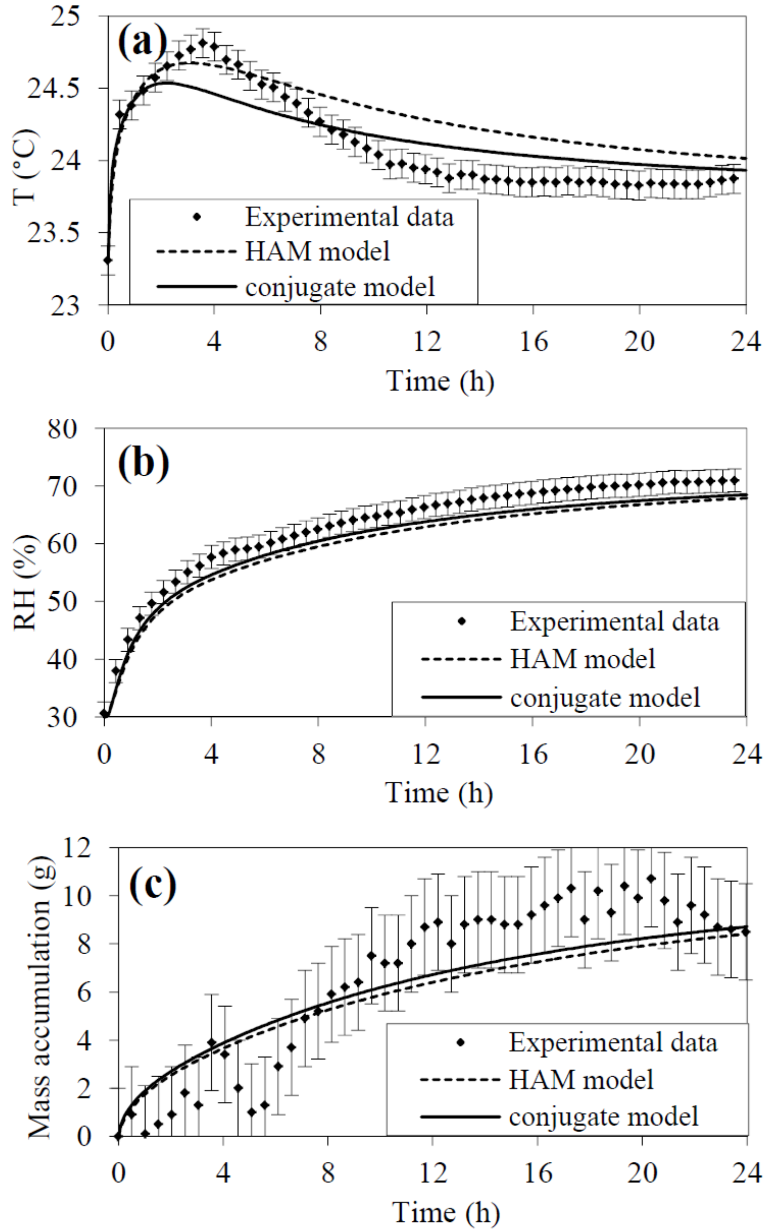


Figure 3. Temperature (a) and relative humidity (b) in the centre of the material below the first gypsum board (x = 250 mm, y = -12.5 mm, see Figure 2) as well as the moisture accumulation in the porous material (c), as a function of time: comparison between experiments (with experimental uncertainty, see James et al. 2010), porous-material simulation with constant CTCs (HAM model) and simulation with the conjugate model.

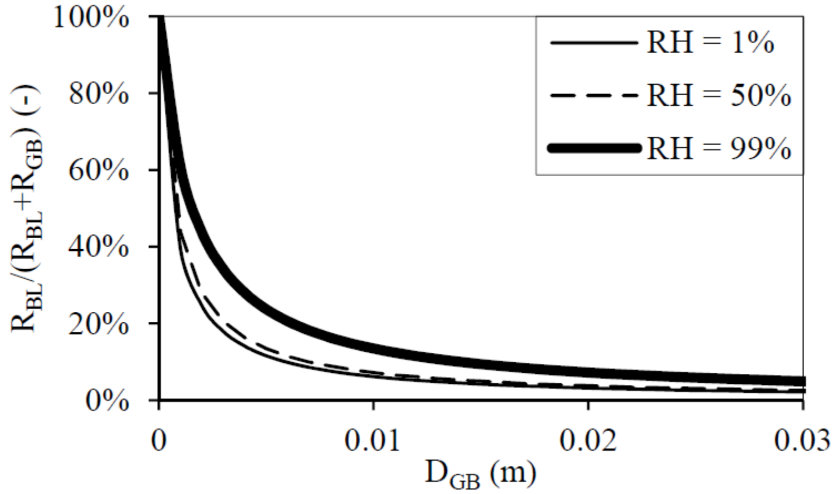


Figure 4. Boundary-layer vapour transfer resistance ($R_{BL}$), normalised with the total resistance of the boundary layer and the gypsum board ($R_{GB}$), as a function of the gypsum board thickness ($D_{GB}$) for different relative humidities of the gypsum board.

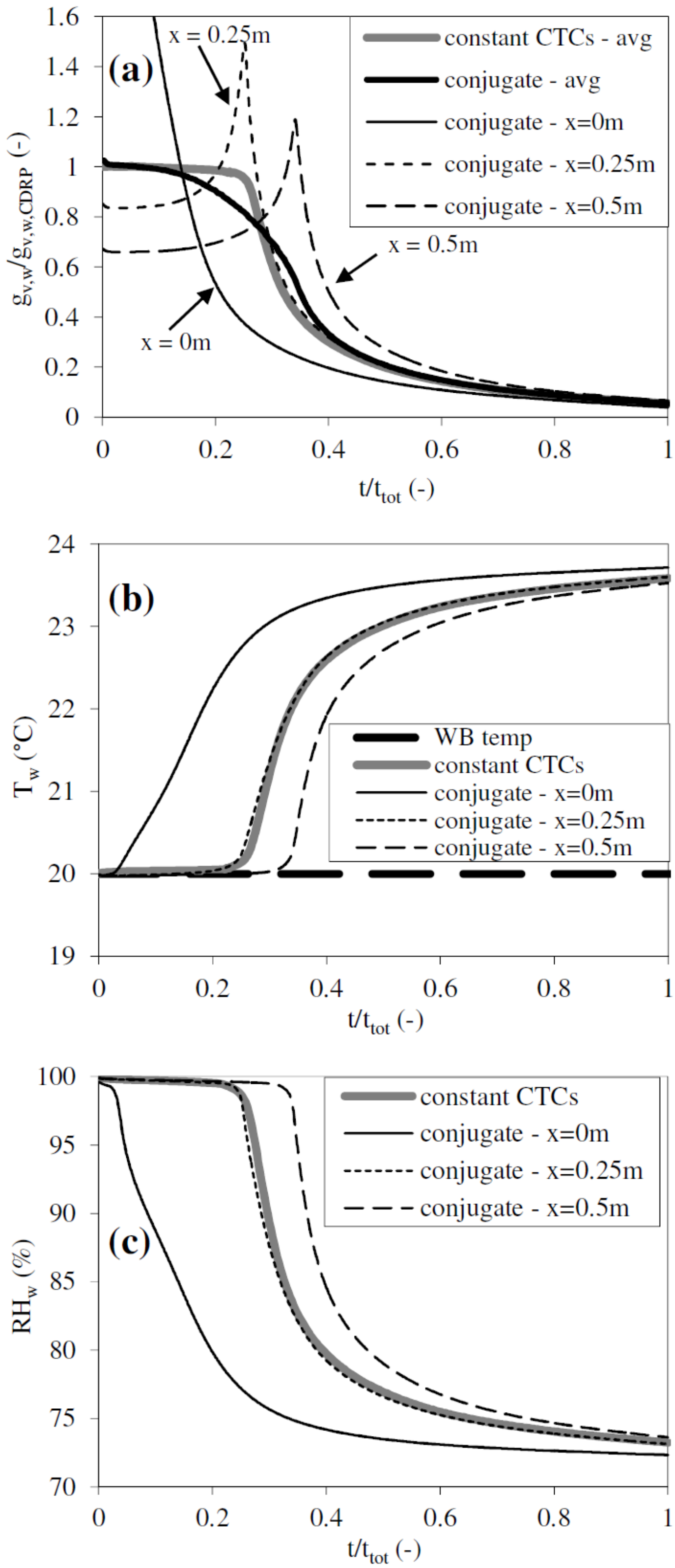


Figure 5. Comparison of two convective boundary-modelling approaches, namely the constant CTC approach and the conjugate approach, from numerical simulations by Defraeye et al. (2012). For the conjugate approach, parameters at specific locations are given. The time is scaled with the total simulation time ($t_{tot}$). (a) Drying rate ($g_{v,w,}$ scaled with $g_{v,w,CDRP}$). The surface-averaged value (avg) for the conjugate approach is also given; (b) Temperature at the interface ($T_w$). The wet bulb temperature is indicated by WB temp; (c) Relative humidity at the interface ($RH_w$).

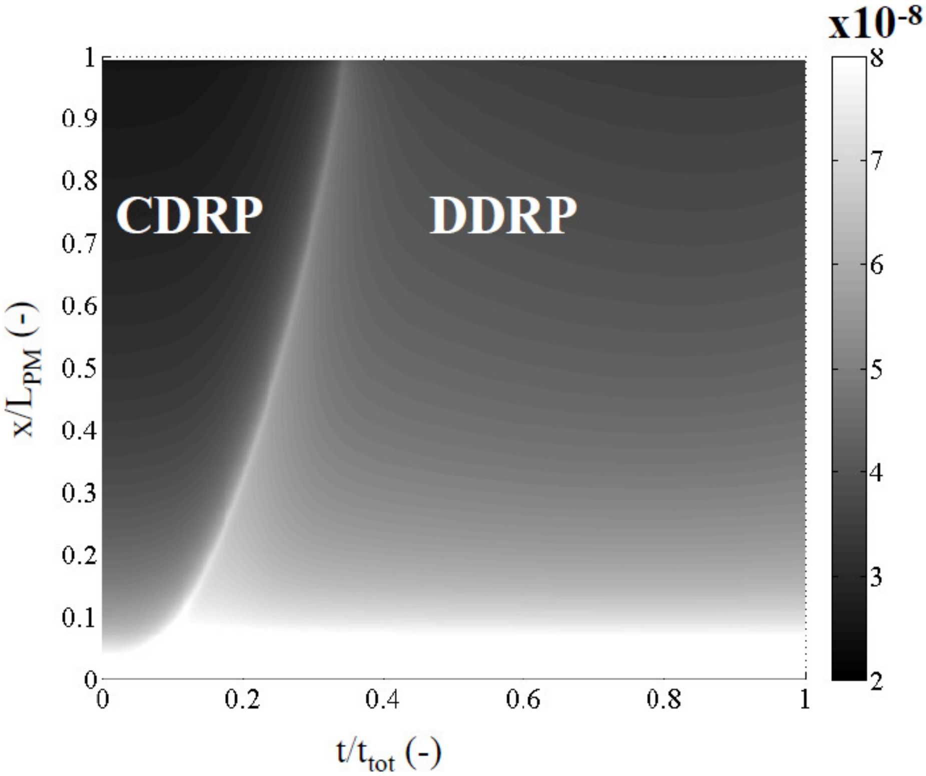


Figure 6. CMTC, as a function of time (scaled with $t_{tot}$) and location on the surface (scaled with $L_{PM}$), calculated according to the conjugate approach, from numerical simulations by Defraeye et al. (2012). The CDRP and DDRP are indicated.

Table 1. Overview of numerical modelling research of porous materials using conjugate convective heat and mass transfer modelling.

| Author(s) | Porous material | Fluid flow | Coupling | Porous material modelling | Fluid flow modelling | Dim. | Validation |
|---|---|---|---|---|---|---|---|
| Chen and Pei (1989) | Wool bobbins, brick slabs and corn kernels, Sat. | ($U_\infty$=2.33-5.25m/s, $T_\infty$=71-80°C) | FC* | SCM (FE) (i) | CTCs (g) | 1D | Yes (b) (d) |
| Masmoudi and Prat (1991) | PM (0.1mx0.1m), Unsat. | Lam. Forc. ($U_\infty$=1m/s, $T_\infty$=25°C) | FC* | H&M TEq. (FE) | CTCs (h) | 2D | No |
| Zeghmati et al. (1991) | capillary PM, Sat. | Lam. Nat. | FC | H&M TEq. (FD) | BL Eqs. (FD) Trans. | 2D | Yes (c) (d) |
| Dolinskiy et al. (1991) | Paper, Sat. | Lam. Forc. ($T_\infty$=90°C) | FC | H&M TEq. (FD) | BL Eqs. (FD) Trans. | 2D | No |
| Oliveira et al. (1994) | Corn meal plate (0.02mx0.02m), Sat. | Lam. Nat. | SC (j) | H&M TEq. (FV) | BL Eqs. (FD) Steady | 2D | No |
| Oliveira and Haghighi (1998) | Wood board sample (0.1mx0.025m), Unsat. | Lam. Forc. (Re=200, $T_\infty$=60°C) | SC | H&M TEq. (FE) | Nav.-Stok. (FE) Steady | 2D | No |
| Suresh et al. (2001) | Brick (0.2mx0.1m), Sat. | Lam. Mix. ($U_\infty$=0.03m/s, $T_\infty$=30°C) | FC | H&M TEq. (FE) | Nav.-Stok. (FE) Trans. | 2D | Yes (a) (d) |
| Murugesan et al. (2001) | Brick (0.2mx0.1m), Sat. | Lam. Mix. ($U_\infty$=0.03m/s, $T_\infty$=20°C) | SC | H&M TEq. (FE) | Nav.-Stok. (FE) Steady | 2D | Yes (a) (d) |
| Erriguible et al. (2005, 2006) | Wood (0.01mx0.01m), Sat. | Turb. Mix. ($U_\infty$=0.5m/s , $T_\infty$=60°C) | FC (f) | H&M TEq. (FE) (i) | Nav.-Stok. (FV) Trans. | 2D | No |
| Kaya et al. (2006) | Rectangular cylinders (apple slices) (0.02mx0.08m), Sat. | Turb. Mix. ($U_\infty$=0.33m/s , $T_\infty$=50°C) | UC | H&M TEq. (FD) | Nav.-Stok. (FV) Trans. vortex shedding | 2D | Yes (d) |
| Younsi et al. (2007) | Wood (0.035mx0.035mx0.2m), Unsat. | Lam. Mix. ($U_\infty$=0.02-1m/s, $T_\infty$=20-220°C) | FC | H&M TEq. (FE) (i) | Nav.-Stok. (FE) Trans. | 3D | Yes |
| Mortensen et al. (2007) | Cellular concrete wall in a room (Thickness 0.1m), Unsat. | Turb. ($U_{inlet}$=0.056-0.33m/s, $T_{inlet}$=20°C) | FC** | H&M TEq. (FV) | Nav.-Stok. (FV) Steady | 3D | Yes (a) (d) |
| Younsi et al. (2008) | Wood (0.1mx0.1mx2m), Unsat. | Turb. Forc. ($U_\infty$=5m/s, $T_\infty$=10-220°C) | FC | H&M TEq. (FD) (i) | Nav.-Stok. (FV) Trans. | 3D | Yes |
| De Bonis and Ruocco (2008) | Rectangular carrot slice (0.06mx0.015m), Unsat. | Lam. Forc. ($U_\infty$=0.3m/s, $T_\infty$ =80°C) | FC | H&M TEq. (FE) | Nav.-Stok. (FE) Trans. | 2D | Yes (d) |
| Lamnatou et al. (2009) | Rectangular cylinder (apple slice) (0.25mx0.05m), Sat. | Lam. Forc. ($U_\infty$=0.33-0.67m/s, $T_\infty$=50°C) | FC | H&M TEq. (FV) | Nav.-Stok. (FV) Trans. | 2D | Yes (a) (d) |
| Steeman et al. (2009a) | Cellular concrete wall in a room (Thickness 0.1m), Unsat. | Turb. Mix. ($T_{inlet}$=11-20.4°C) | FC | Heat TEq. (FV) - Mass EPDM | Nav.-Stok. (FV) Trans. | 2D/ 3D(e) | Yes (c) (d) |
| Steeman et al. (2009b) | Microclimate vitrine for paintings, Unsat. | Lam. Nat. | FC (k) | H&M TEq. (FV) | Nav.-Stok. (FV) Trans. | 3D | Yes (d) |
| Lamnatou et al. (2010) | Rectangular cylinders (apple slices) (0.25mx0.05m), Sat. | Lam. Forc. (Re=463& 926, $T_\infty$=50°C) | FC | H&M TEq. (FV) | Nav.-Stok. (FV) Trans. | 2D | Yes (a) (d) |
| Chandra Mohan and Talukdar (2010) | Rectangular cylinder (0.02mx0.02mx0.08m), Sat. | Lam. Forc. ($U_\infty$=0.1-0.3m/s, $T_\infty$=40-80°C) | UC | H&M TEq. (FV) | Nav.-Stok. (FV) Steady | 3D | Yes (b) (d) |
| Defraeye et al. (2012) | Mineral plaster plate (0.5mx0.0375m), Unsat. | Lam. Forc. (Re=1100, $T_\infty$=23.8°C) | FC (f) | H&M TEq. (FE) | Nav.-Stok. (FV) Trans. | 2D | Yes (a) (l) |

**BL Eqs.**: Boundary-layer equations, **Dim.**: Dimension (1D, 2D, 3D), **EPDM**: Effective Penetration Depth Model, **FC**: Full coupling (PM and flow field are both solved each time step), **FC***: Full coupling (PM and CTCs are both solved each time step, where CTCs are dependent on PM conditions), **FC****: Full coupling (PM and flow field are both solved but in steady state), **FD**: Finite Difference method, **FE**: Finite Element method, **FV**: Finite Volume method, **Forc.**: Forced convection, **H&M**: Heat and mass transfer, **Lam.**: Laminar flow, **Mix.**: Mixed convection, **Nat.**: Natural convection, **Nav.-Stok.**: Navier-Stokes equations, **PM**: Porous material, **Sat.**: Saturated PM, **SC**: Semicoupled (Fluid flow is solved assuming a quasi-steady flow field but transport of heat and moisture in the flow field is calculated every time step, as well as the PM), **SCM**: Shrinking Core Model, **Steady**: Fluid flow is assumed to be quasi-steady and is thereby taken constant in time and is thus not coupled with the PM calculation and is consequently only solved once (i.e. not every time step), **TEq.**: Transport equations, **Trans.**: Transient flow calculation (i.e. performed for each time step), **Turb.**: Turbulent flow, **UC**: Uncoupled approach (CTCs from separate CFD simulation and these are afterwards transferred to porous-material model), **Unsat.**: Unsaturated PM; (a): Validation was performed separately for the flow field and the PM, (b): Validation was only performed for the porous material, (c): Validation was only performed for the flow field, (d): Validation was performed with data from other researchers, (e): 3D for flow and 2D for PM, (f): PM and flow field are solved using two different programs where BC information is exchanged between programs every time step, (g): CTCs vary with the moisture content in the decreasing drying rate period, (h): Local CTCs obtained with superposition method (Kays and Crawford 1993, pp. 175-178) for each time step, (i): Bound water taken into account, (j): PM and flow field are solved using two different programs where during each time step iterations are performed between both programs until convergence is reached within that time step, (k): Radiation is taken into account, (l) Validation of the models that are used was performed in previous studies.